INCORPORATION OF NEWLY FORMED LECITHIN INTO PERIPHERAL NERVE MYELIN

R. M. GOULD and R. M. C. DAWSON

From the Neurochemistry Department, Institute for Basic Research in Mental Retardation, Staten Island, New York 10314 and the Biochemistry Department, Agricultural Research Council, Institute of Animal Physiology, Babraham, Cambridge CB2 4AT, England

ABSTRACT

Radioactive choline was used to study the metabolism and movement of choline-containing phospholipids in peripheral nerve myelin of adult mice. Incorporation at various times after intraperitoneal injection was measured in serial segments of sciatic nerve as well as in myelin isolated from those segments. At no time (1 h to 35 days) could a proximal-distal difference in the extent of labeling be demonstrated. This finding suggests that incorporation of precursor choline phospholipids into nerve membranes is a local event, with little contribution from the neuronal perikaryon via axoplasmic transport.

Autoradiographic investigations were undertaken to elucidate the pattern of movement of radioactive choline-labeled phospholipids, predominantly lecithin, into the myelin sheaths of the sciatic nerve. A sequence of autoradiographs was prepared from animals sacrificed between 20 min and 35 days after a microinjection of precursor directly into the nerve. Analysis of these autoradiograms revealed that labeling is initially concentrated in the Schwann cell cytoplasm. Later, the label moves first into the outer regions of the myelin sheaths and is eventually distributed evenly throughout the inner and outer layers of the sheath. At no time is there a build-up of label in the axon.

The rate of uptake of precursor and subsequent redistribution of lecithin into the myelin were also examined in frog sciatic nerve (18°C). Both uptake and redistribution processes were considerably slower in the cold-blooded animal.

Various metabolic studies (15, 57) have shown that the sequence of events responsible for the dynamic turnover of membrane phospholipid (and protein) components includes synthesis in the endoplasmic reticulum and subsequent translocation to a variety of other membrane structures. Many recent reports have supported the contention that a turnover of myelin phospholipids occurs in the brain of adult animals (e.g. 9, 28, 29, 50). Miller and Dawson (34), employing subcellular fractionation of brain, have shown that most phospholipid biosynthesis including that of phosphatiylcholine takes place in "microsomes," with no activities detectable in isolated mitochondria or myelin. In addition, these authors (35) were unable to detect any component in brain cytoplasm which could

assist the transfer of phospholipids from "microsomes" to "myelin," although there are protein factors in brain supernate that catalyze the transfer to phospholipids between "microsomes" and "mitochondria." Histochemical studies by Benes and co-workers (8) have indicated different subcellular structures in the Schwann cell as sites of lipid acylation. One question which, therefore, arises is where and how does the myelin sheath obtain the phospholipids deposited during its formation and growth, and subsequent turnover.

We have chosen autoradiography to examine these questions with respect to choline-phospholipids. It has been well documented that [^{3}H]choline is a suitable precursor for autoradiographic studies (12, 27, 52, 53, 55). Hendelman and Bunge (27) used [^{3}H]choline with myelinating tissue cultures of peripheral nerve to ascertain whether metabolic processes active during myelin formation have a continuing role in maintenance and repair of "mature" myelin. They chose peripheral nerve, as have we, because of morphological considerations; the one-to-one relationship between Schwann cell and myelin internode, and the large extracellular areas that accommodate collagen fibers, facilitate the statistical evaluation required in autoradiographic analyses. However, our investigation focuses on in vivo metabolism in the mature animal, thus allowing more detailed analyses of the autoradiograms, so that the movement between the myelin lamellae might be considered. In adult animals the proportion of large-caliber fibers is increased (20, 21), and it is these fibers that give us information on the rates of movement of the labeled phospholipids through the sheath. In a study of cholesterol incorporation into the myelin sheath of developing animals, Rawlins (38) used an analysis of this sort to show that cholesterol enters the myelin sheath rapidly from both the inner and outer lamellae. In contrast to this rapid movement observed for cholesterol, Rawlins (39) has recently reported by autoradiography that ^{3}H-choline-labeled molecules move very slowly into the myelin sheath of adult mice both from the outer Schwann cell cytoplasm and, to a markedly lesser extent, from adaxonal Schwann cell cytoplasm. That report was in substantial agreement with a preliminary one from our own laboratory (24), where a slow movement of [^{3}H]lecithin from sites of synthesis in Schwann cell cytoplasm into myelin was also demonstrated. In the present communication, by both biochemical and autoradiographic studies, we document the slow rate of movement of lecithin through the myelin sheath and suggest that lateral diffusion may be rate-limiting in this process.

MATERIALS AND METHODS

Young adult mice (45–150 days) were used. Frogs (*Rana temporaria*) were examined in some autoradiographic experiments.

Total-Animal Labeling and Sampling of Nerves for Biochemical Examination

Radioactive [*methyl*-^{3}H]choline (spec act 10 Ci/nmol, The Radiochemical Centre, Amersham) was injected intraperitoneally at a concentration of 1 mCi/ml (0.05 or 0.2 ml) in sterile saline. Radioactive phosphate (95 Ci/ng P) was injected likewise, 200 μCi ^{32}Pi per mouse. At each of various time intervals after injection, several animals were anesthetized with ether and decapitated. Both sciatic nerves were dissected between the point where they leave the spinal cord and the trifurcation in the lower thigh. Nerves were slightly stretched onto index cards and were cut into six or seven 3-mm segments from the proximal end. Segments from the left nerve and random segments from spinal cord and liver were removed and homogenized in 5 ml of chloroform:methanol, 2:1 vol/vol. A Folch et al. extraction (19) and washings were carried out to separate an upper (aqueous-methanol) and lower (chloroform-rich) phase. The upper phase was dried, resuspended in 1 ml of water, and counted in 10 ml of Unisolve scintillation fluid (Koch Light, Colnbrook, Bucks). The lower phase was divided into two portions, one of which was analyzed for lipid phosphorus (7) and the other which was dried and counted in a toluene-based liquid scintillation mixture.

Isolation of myelin was carried out by a procedure similar to one described by Norton and Poduslo (36). The segments (taken in pairs from the proximal end, i.e. 3 of 6 mm) from the right sciatic nerve were each homogenized in a motor driven, all-glass, 1-ml homogenizer (Kontes Glass Co., Vineland, N. J.) in 0.3 M sucrose containing 10 mM Tris-HCl, pH 7.3. Sciatic nerve and spinal cord homogenates, 1–2 ml, were layered on a discontinuous gradient (6 ml of 0.32 M sucrose over 8.5 ml of 0.85 M sucrose) and were centrifuged at 75,000 *g* for 30 min in an SW 27 Rotor (Beckman Instruments, Inc., Spinco Co., Palto Alto, Calif.). The myelin interface was collected, homogenized in 15 ml of distilled water, and pelleted at 15,000 rpm for 15 min (SS-34 Sorvall Rotor, Dupont Instruments, Sorvall Operations, Newtown, Conn.). The myelin pellet was resuspended in distilled water and washed twice by centrifugation at 10,000 rpm for 10 min. The supernate above the myelin interface and the supernate of the first water shock were pooled and pelleted at 40,000 rpm (105,000 *g*) for 90

min to give a "microsomal" pellet. The 0.85 M "mitochondria-rich" pellet from the initial gradient was also saved. Subfractions pelleted from distilled water were extracted with chloroform-methanol and analyzed in the same manner as described above for the whole-nerve segments.

Direct Nerve Labeling and Processing for Autoradiography

Mice were anesthetized with halothane gas. The sciatic nerve was exposed in the mid-thigh region and 0.1–0.2 μl of radioactive [*methyl*-^{3}H]choline (spec act 10–16.5 Ci/nmol) in sterile saline was injected slowly into the nerve according to the procedure of Hall and Gregson (25). The animals were awake and active within 2–5 min of the injection and showed no impairment in movement from within a few hours of surgery up to time of killing.

Frogs were anesthetized in a solution of 0.35% of MS-222 (Sandoz Inc., Hanover, N. J.) in tap water and the sciatic nerve was exposed and injected in the same way as the mice. After injection, the animals were rinsed in cold water; they recovered completely within 30 min to 1 h and were kept in an aquarium at 18°C showing no impairment of movement in the operated leg up to time of sacrifice.

At appropriate times after injection, animals were sacrificed and segments of nerve around the injection (6–8 mm) were dissected and immersed in a fixative of 3% glutaraldehyde prepared Millonig's buffer, pH 7.2 (26) containing approximately 2 mM choline chloride, and 2 mM phosphorylcholine, calcium salt. The nerves were fixed for 2–4 h at 0–4°C and subsequently washed by immersion in buffer at 0–4°C for 2 days. Nerve was postfixed in 1% osmium tetroxide, buffered with Millonig's buffer for 1 h, and dehydrated at room temperature for 10 min each in 50%, 75%, and 100% acetone (three times). After a 15-min wash with propylene oxide, the nerves were immersed for 4 h in TAAB embedding resin (TAAB Laboratories, Reading, England) and then embedded in this resin. After overnight infiltration, blocks containing the nerve were polymerized at 60°C for 24–48 h.

Procedures Developed to Retain Labeled Lipid but not Water Precursors during Fixation and Embedding

After microinjection, radioactive precursors are present in the nerve at high levels. To assist in removing these, unlabeled choline and choline phosphate were included in the fixative and buffer. Repeated washings during 2 days proved necessary to reduce water-soluble radioactivity to well below that of lipid (Table IB). Little organic-solvent extractable radioactivity was liberated during these extended washings. During the subsequent postfixation, dehydration, and embedding steps, losses of radioactive lipid were never greater than 10%. Acetone dehydration limited extraction of lipid radioactivity to 10–20% of that occurring during ethanol dehydration. Other workers have already noted that phospholipids in myelin are insensitive to acetone dehydration (2, 11, 42). Low viscosity, TAAB-embedding resin infiltrated the tissue rapidly and effectively without solubilizing radioactive lipid (Table IA). Both epon and araldite, which were initially used as embedding agents in conjunction with propylene oxide, caused considerable extraction of lipid-soluble radioactivity.

Osmium tetroxide postfixation was used routinely. Although this treatment makes only a small percentage of the radioactive lipid insoluble in chloroform to methanol (C vs. B), appreciable interaction of osmium with soluble lipid takes place. When the chloroform to methanol soluble material is chromatographed on thin layer, the label migrates slower than nonosmium-treated control. This postfixation apparently reduces displacement of the lipid in the tissue during dehydration and/or embedding (Dr. Paul H. Patterson, Harvard Medical School, personal communication), but leads to a negative chemography by causing bleaching of silver grains over myelin tracts. This chemography could only be eliminated with an intervening carbon film between tissue and emulsion.

In summary, the bulk of the radioactivity in the embedded tissue is associated with lipid and not with water-soluble metabolites. During fixation, dehydration, and embedding procedures, water-soluble precursors are selectively removed from the nerve (Table ID).

Preparing Autoradiographs for Light and Electron Microscope

Segments of nerve 1–2 mm long were oriented to cut transverse sections. For the mouse, sciatic nerve samples taken from animals at 20 min, at 1, 2, 4, and 6 h, and at 1, 4, 19, and 35 days after injection were prepared. For the frog, samples taken at 4 and 8 h, and at 1, 4, 8, and 15 days after injection were prepared.

Several animals had been injected for each sampling time. Light and electron microscope autoradiographs were prepared from one or two segments of nerve from each animal. Analyses were limited to one animal based on (*a*) high ratio of lipid to water-soluble counts in tissue, (*b*) adequate radioactivity in the tissue, and (*c*) good tissue morphology.

For light microscope autoradiography 0.5–1 μm thick sections were cut and transferred to glass microscope slides. These slides were carbon coated before dipping in a 1:1 dilution of Ilford K-2 nuclear emulsion. Several exposures were made for each tissue block. After exposure for 1 wk to 4 mo, slides were developed with Phen-X developer and then stained with 1% Azur 11 in distilled water.

TABLE I

Extraction of Lipid and Water Soluble Radioactivity during Fixation, Dehydration and Infiltration

Mouse sciatic nerve	Fixed at 20 min after [^{3}H]choline inj.	Fixed at 35 days after [^{3}H]choline inj.
	dpm	*dpm*
(A) Radioactivity liberated into solutions:		
Glutaraldehyde fixative (2 h)	1,064,670	45,470
Buffer washes	148,440	19,000
Acetone, propylene oxide dehydrations	2,050*	730*
TAAB embedding resin	300*	120*
(B) Distribution of radioactivity in fixed tissue after 2 days washing (2 mm analyzed)		
Chloroform phase	41,500 (97%)	64,080 (91%)
Aqueous phase	1,190 (3%)	5,980 (9%)
Chloroform:methanol extracted pellet	20	20
(C) Distribution of radioactivity in fixed tissue after washes, postfixation in osmium tetroxide, dehydration, and infiltration (2 mm analyzed)		
Chloroform phase	32,910 (75%)	57,330 (94%)
Aqueous phase	2,500 (6%)	1,380 (2%)
Chloroform:methanol extracted pellet	8,330 (19%)	2,590 (4%)
(D) Estimations of lipid and aqueous radioactivity in embedded tissue (based on total 6 mm length)		
Chloroform phase	125,000* (95%)	182,000* (96%)
Aqueous phase	6,000* (5%)	8,000* (4%)
% of Radioactive lipid extracted	2.0%	0.5%
% of Aqueous label extracted	99.5%	89%

* Calculations made for 6 mm length of nerve assuming equal distribution of radioactivity along the nerve.

Sciatic nerve segments between 6–8 mm long were dissected from mice after 20 min and 35 days and were immersed in fixative for 2 h (4°C). During the procedure portions of fixative solution and various washes were either counted directly (A) or after separation into aqueous and organic soluble fractions. Radioactivity in the dehydrating and infiltrating solutions are corrected for segments removed (A). After the buffer washes, 1-mm pieces were cut from the ends of each nerve homogenized in chloroform:methanol (B). An insoluble residue was separated by centrifugation. The residue was reextracted with chloroform:methanol. The pooled chloroform:methanol extract was washed with saline and portions of upper aqueous and lower chloroform phase were counted. The residue was solubilized in NCS solubilizer and counted.

The remaining nerve was postfixed in 1% buffered osmium tetroxide, dehydrated with acetone and infiltrated with TAAB embedding resin. Before polymerization additional 1-mm pieces were severed (C) from the tissue and extracted as described above. The remaining 2 mm of each nerve were embedded for the autoradiographic study.

Estimations of radioactivity in total 6 mm of nerve (D) were used to calculate percentages of radioactive lipid and water-soluble precursors extracted during fixation, dehydration, and infiltration. These calculations were based on the observations that radioactivity in the fixative solution and buffer wash is largely water soluble and radioactivity extracted into the acetone and TAAB resin is largely chloroform soluble (A). Percentage values (given in parentheses) express the distribution of label in fixed nerve between chloroform soluble, aqueous soluble, and chloroform:methanol insoluble.

For electron microscopy, sections colored pale gold to gold by interference were cut and placed on 0.8% collodion-coated microscope slides. The sections were stained for 10 min with 2% uranyl acetate in 0.1 M maleate buffer pH 4.2, and for 1–4 min with Reynolds lead citrate (40). After carbon coating, the sections were covered, by a dipping procedure, with a monolayer of Ilford L-4 nuclear emulsion; these were exposed at 4°C for periods of 2 wk to 4 mo and developed with freshly prepared ID 19 developer for 3 min. Several exposures

were made for each tissue block. The collodion layer was then floated onto a water surface, grids were placed over the sections, and the film was picked up onto filter paper and dried. Uninjected and saline-injected nerves were used as controls to evaluate background. Some experimental slides were fogged before development to test latent image fading. With carbon coating of slides, and exposures in light-tight boxes at −20°C, the background radioactivity was very low (usually less than 1 grain/500 μm^2), and no negative chemography or latent image fading was observed, even in exposures of 4 mo.

Although most grids were prestained with both uranyl and lead stains, some experimental slides were exposed without prestaining. Poststaining procedures were only successful after washing the grids with butan-1-ol for 3 min. Quantitative analysis of these poststained grids demonstrated grain densities identical to the prestained grids.

Analysis of Electron Microscope Autoradiographs

Grids containing labeled sections were examined with either a Siemans Elmiskop 1A or a Philips 300 electron microscope. Areas were selected having the least amounts of other cellular structures, such as large blood vessels and perineurium, and were photographed at a constant magnification of 3,000. Prints were made of negatives containing between 30 and 250 grains on 8 × 10 in or 11 × 14 in paper at a final magnification of 10,000.

Photographs containing between 50 and 200 grains were chosen for analyses. Between 8 and 18 photographs were analyzed for each sampling time (4,000 μm^2–10,000 μm^2, total area). Greater than 800 grains and circles were used in each analysis and were classified into primary and junctional items (Table II) according to the procedure of Williams (55, 56). The "random circle" grids employed in the analyses had a diameter of 2.5 mm and were placed in a quatratic array 15 mm apart on a sheet of clear stiff plastic (16 columns × 13 rows). At a magnification of 10,000, these circles (diameter of 2,500 Å) surrounded most of the developed grains. Their size was chosen to reduce the percentage of grains classified in junctional areas and maximize the number of subdivisions of the large caliber myelin fibers, although they had only a 25–30% probability of enclosing a point source (56).

Only grains circumscribed with circles, or circles lying exclusively over myelin, were classified in one of the myelin subclassifications (1 to 5). Grains associated with myelin were classified arbitrarily in category 1 if their centers were within 2.5 mm of the myelin/Schwann cell interface or myelin/extracellular space interface, in category 2 if their centers were between 2.5–5.0 mm from the outer myelin lamellae, in category 3 with centers 5.0–7.5 mm from the outer lamellae, etc. The small percentage of grains found lying over Schmidt-Lantermann clefts or between these clefts and the myelin/axon boundary were not subclassified, but only classified as originating from the myelin. The higher proportion of random circles found in categories 1 and 2, compared with 3, 4 and 5 reflect the contribution of small caliber fibers which would not possess higher numbered categories. The greater proportion of random circles in category 2 vs. 1 reflects the junctional regions (myelin/Schwann and myelin/extracellular) which reduce the number of circles (and grains) considered in category 1 (Table II). The grain densities (G/C) were tabulated after normalizing total grains (G) to equal total random circles, and Chi-square analyses were carried out to assess the significance of the distributions (6, 55, 56).

RESULTS

Comparison of Phospholipid Labeling in Liver and Nervous Tissue after Intraperitoneal Injection of Precursors

^{32}Pi labeling (Table III) of liver phospholipids peaked rapidly and declined over the following days, commensurate with rapid turnover and exhaustion of radioactive precursor (not shown). Labeling of nervous-tissue phospholipids was markedly poorer than that of liver; the specific radioactivity became maximal only after some days. When the sciatic nerve tissue was subfractioned on a discontinuous sucrose gradient, phospholipid labeling of the myelin fraction was considerably slower than that of whole nerve and other fractions, although by 8 days labeling of myelin matched that of nerve phospholipids (see also Fig. 1).

Tritiated choline (Table IV) was also incorporated into nervous tissue phospholipids much more poorly than into liver. Whereas the extent of labeling in liver peaked by 1 day postinjection, the labeling of myelin-rich nervous tissue took longer to become maximal. Even after 34 or 35 days, when the levels of label in liver and blood were extremely low, label persisted in nervous tissue to at least 25–33% of maximum. Some variation in labeling may be due to differences in the ages of the animals at the time of injection (Table IV). The lower labeling in nerves and cord of the 2, 4, and 8 day, vs. 1 day animal, may reflect a decreased metabolic rate in the older animals (50).

An examination of myelin from central and peripheral nerve showed that labeling in these structures was retarded compared with other subfractions or whole nerve. However, by 8 days, label in myelin phospholipids approached that in whole

TABLE II

Results Derived from Two Sets of EM Autoradiographs Analyzed by the Method of Williams (55, 56)

Item	Mouse 20 min after [³H]choline injection					Mouse 35 days after [³H]choline injection				
	Actual no. of silver grains (G)	Actual no. of random circles	Expected no. of grains if random (C)	Grain density (G/C)	χ^2 Chi-square $(G-C)^2/C$	Actual no. of silver grains (G)	Actual no. of random circles	Expected no. of grains if random (C)	Grain density (G/C)	χ^2 Chi-square $(G-C)^2/C$
Column:	1	2	3	4	5	1	2	3	4	5
1. Axon	31	398	173	0.18	116.6	119	271	264	0.45	79.6
2. Myelin	136	535	233	0.58	40.4	866	364	355	2.44	735.6
3. Schwann cytoplasm (SC)	178	57	25	7.12	936.4	27	45	44	0.61	6.6
4. Schwann nucleus (SN)	7	10	4	1.75	2.2	5	18	18	0.28	9.4
5. Unmyelinated fibers (UMF)	15	31	13	1.15	0.3	12	51	50	0.24	28.9
6. Other cells (OC)	0	0	0	0	0	14	5	5	2.8	16.2
7. Extracellular space (ECS)	153	385	167	0.92	1.2	133	541	527	0.25	294.6
8. SC/ECS	112	104	45	2.49	99.8	40	68	66	0.61	10.2
9. Myelin/ECS	33	101	44	0.75	2.8	116	88	86	1.35	10.4
10. Myelin/SC	96	84	36	2.67	100	144	80	78	1.85	55.8
11. Myelin/axon	16	137	59	0.27	31.3	152	117	114	1.33	12.7
12. SC/SN	21	4	2	5.25	72.2	2	11	11	0.18	7.4
13. UMF/ECS	6	9	4	1.50	1.0	7	16	16	0.43	5.1
14. OC/ECS	0	0		0	0	0	4	4	0	4.0
Myelin subclasses										
1 (outer)	66	140	61	1.08		204	112	109	1.87	
2	48	177	77	0.62		379	145	141	2.69	
3	16	127	55	0.29		214	80	78	2.74	
4	0	59	30	0.07		55	20	24	2.83	
5 (axonal, inner)	2 (2)	11 (70)				13 (68)	5 (25)			
Totals (excluding subclasses)	804	1,855	805		1,404.2	1,637	1,679	1,638		1,276.5

The categories selected for the analyses of electron microscope autoradiographs are shown at the left. Numerical results are listed in the succeeding columns for two separate analyses of mouse nerve, an early time of 20 min after injection and a later one of 35 days. The first analysis includes the total grains and random circles identified in nine photographs produced at 10,000 final magnification. The second includes results from eight photographs. Chi-square tests of significance (column 5) demonstrate that the grains are nonrandomly distributed over the photographs.

TABLE III

Specific Activities of Phospholipids in Tissues and Subfractions after Injection of ^{32}Pi(i.p.)

Time after injection	Tissue			Sciatic nerve subfractions	
	Liver	Spinal cord	Sciatic nerve	Myelin	Pellet
		(*dpm/μg lipid P*)		*% of total homogenate*	
3 h	46,600 ± 1,055 (2)	1,221 ± 418 (2)	846 ± 250 (6)	45	115
2 days	20,950 ± 1,505 (2)	3,942 ± 2,505 (2)	3,305 ± 276 (6)	63	88
4 days	18,150 ± 1,039 (2)	3,630 ± 184 (3)	2,962 ± 163 (6)	72	161
8 days	9,682 ± 140 (2)	5,009 ± 28 (2)	4,680 ± 301 (6)	96	89

Four female mice were each injected i.p. with 200 μCi of ^{32}Pi (spec act at time of injection, 95 Ci/mg phosphorus). At 3 h (23.2 gm), 2 days (26.6 g), 4 days (33.4 g), and 8 days (16.5 g) one animal was weighed and sacrificed. Values for the tissue are recalculated to an animal weight of 25 g. Error is calculated as standard deviation for numbers of tissue samples enclosed in parentheses. Values for the sciatic nerve subfractions (left leg) are averages of three samples each and are expressed as percentages of total sciatic nerve homogenate (determined on right leg).

TABLE IV

Activity of Choline Phospholipids in Tissue and Subfractions after Injection of Radioactive Choline (i.p.)

Time after injection	Tissue				Subfractions							
					Myelin		Microsomes		Pellet			
	Blood	Liver	SC	SN	SN	SC	SN	SC	SN	SC	Age	Wt.
	(*dpm/μg lipid phosphate*)				(*% of total tissue activity*)						*days*	*g*
10 h	—	12,068 ± 2,097	172 ± 47	227 ± 97	1	37	13	88	39	354	67	38.5
1 day	—	29,031 ± 5,099	600 ± 108	522 ± 94	27	54	57	22	37	163	68	33.1
2 days	5,134 ± 692	5,458 ± 452	279 ± 58	106 ± 32	46	32	490	149	261	189	118	43.6
4 days	4,156 ± 779	3,274 ± 1,095	442 ± 84	215 ± 175	39	32	34	40	67	161	120	39.6
8 days	2,211 ± 256	1,423 ± 371	445 ± 50	193 ± 39	93	60	33	31	41	201	124	43.7
34 days	230 ± 40	53 ± 4	312 ± 35	260 ± 66	120	105	78	52	31	125	78	40.2
35 days	178 ± 40	40 ± 22	156 ± 18	172 ± 34	103	74	47	48	46	143	79	37.8

Male mice (2–4 mo old) were injected intraperitoneally with 200 μCi of [*methyl*-^{3}H]choline (spec act 10 mCi/mmol). At indicated times after injection one animal was killed and tissues were dissected and prepared as described in methods. Standard error calculations for tissue were based on six sciatic nerve segments, three spinal cord and liver samples, and two blood samples. For the subfraction results are expressed as percentages of activity in tissue homogenates. Ages and weights are recorded at time of sacrifice. Tissue values are normalized to an animal of 35 g at time of death.

nerve in both CNS and PNS tissue (See also Fig. 1). Label persisted in the myelin; at 35 days, it remained at near maximal levels. By this time the radioactivity in the other subfractions (on a percentage-of-total-homogenate basis) was significantly lower than at earlier times and in myelin.

Phospholipid Labeling along Sciatic Nerve after Intraperitoneal Injection of Phospholipid Precursors

One possible explanation for the retarded incorporation of precursor phospholipid into both PNS and CNS myelin could be the limitations imposed by a slow axoplasmic transport from sites of synthesis in the neuron to the myelin sheath. In order to investigate this possibility incorporation of label into the peripheral nerve and myelin subfraction was examined along its length.

The intraperitoneal route is not the best for obtaining good labeling of nervous tissue (28); especially charged precursors such as phosphate and choline penetrate the tissue rather slowly. However, one advantage of this route is that it probably does not favor labeling in peripheral neuronal perikarya of spinal cord and dorsal root ganglia over glial cells along the nerve. Both fast- and slow-transport systems are characterized by the labeling of proximal (closer to the cell body) before distal portions of the nerve (13, 33). Thus,

transport of phospholipids to myelin should be apparent, at some appropriate time after a pulse, as a higher labeling in proximal relative to distal portions of the nerve. By use of both ^{32}Pi and [^{3}H]choline as precursors, the distributions of label in sequential segments of nerve and myelin isolated from corresponding segments were examined (Fig. 1). At 2 days after the injection, the phospholipid labeling of the total nerve segment was high compared to that of myelin with both precursors. By 8 days, the activity (μg lipid P) in segments of the whole nerve had increased marginally, while the activity in the myelin phospholipids had increased to almost the same level, indicating movement of labeled lipid into myelin from other membranes of the nerve. No major differences were seen between proximal and distal areas, at these times or at the other times examined (from Table III and IV).

Labeling of Phospholipids in the Nerve Fibers after Local Injection

The levels of radioactive lipid present in mouse sciatic nerve after intraperitoneal injection of precursor proved insufficient for autoradiographic study. Local injection of [^{3}H]choline into the nerve proved satisfactory for autoradiography, but did not give reproducible levels of incorporation, probably because of variations in tissue geometry and blood supply, rate and amount of material injected, and a certain amount of unavoidable back leakage. Because of this difficulty, no attempt was made to determine absolute grain density changes in relation to the sampling time. The highest labeling was always recorded at the site of the needle tip, with a sharp drop at about 3–4 mm on either side of the injection site.

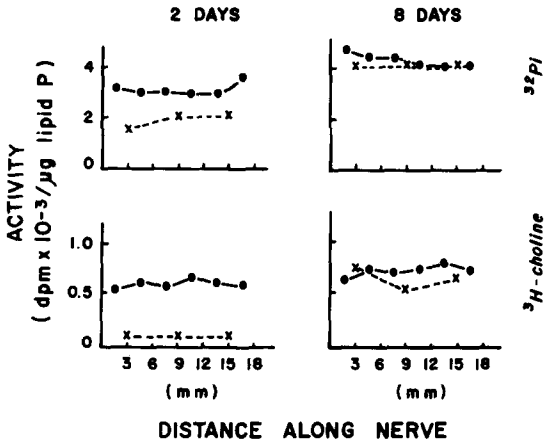

FIGURE 1 Distribution of radioactive lipids along length of nerve and myelin after intraperitoneal injection of precursors. Mice were injected with [^{32}P]inorganic phosphate (upper graphs) or [^{3}H]choline (lower graphs) precursors. After 2 and 8 days animals were sacrificed and the activities on a μg lipid phosphate basis were measured from lipid isolated from consecutive 3-mm segments removed from the right sciatic nerve (●—●). Myelin was isolated from 6-mm segments of the left nerve, and activities were measured of lipid extracted from the washed myelin pellet (x---x). The initial segments (0–3 mm) begin within 1–2 mm from where the spinal nerves leave the vertebrae of the cord and continue in a distal direction.

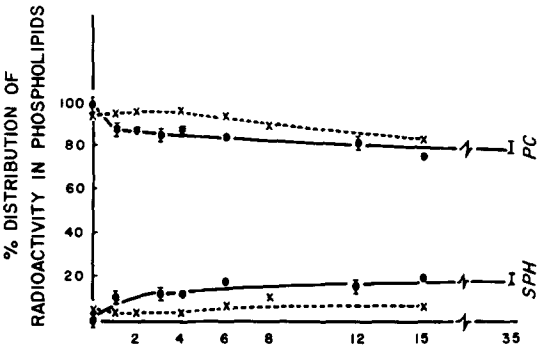

FIGURE 2 Distribution of radioactive choline in phospholipids after microinjection. Labeled [^{3}H]choline was introduced into the sciatic nerve of both mice and frogs by a microinjection procedure. The animals were sacrificed and 6-mm segments around the site of injection were removed and fixed in glutaraldehyde. 2-mm segments from each end of the nerve were removed after washing the nerves in buffer, and were homogenized in chloroform:methanol (2:1 vol/vol). After two Folch washes (18), portions of the chloroform phase were spotted on silica gel H plates and chromatographed (chloroform:methanol:7N ammonium hydroxide: (69:27:4.5). All radioactivity was recovered in spots corresponding to lecithin (PC) and sphingomyelin (SPH). After subtraction of blanks, percentage distributions were calculated and were plotted for both mouse nerve (●—●) and frog nerve (x---x). Vertical bars represent spread between two separate nerve segments from the same animal.

Lipid-soluble radioactivity in mouse nerve was predominantly in lecithin, greater than 95% in the first hours, and around 80% at later times (Fig. 2). Even after the longest time period, 35 days after injection, the distribution of label between lecithin (80%) and sphingomyelin (20%) remained more or less as at 12 days, although in peripheral nerve (45)

and peripheral myelin (37, Gould, Jacobson and Dawson, unpublished), the levels of sphingomyelin have been demonstrated to be higher than or equal to the levels of lecithin. The preferential labeling of lecithin compared with sphingomyelin was even more pronounced in frog sciatic nerve (Fig. 2).

Observations of Labeling Patterns from Light and Electron Microscope Autoradiographs

Autoradiographs were prepared from nerves fixed at various times after local injection of [^{3}H]choline. It was hoped that very short times would localize the sites of radioactive choline incorporation into lecithin, and that later times would provide information on slower processes involved in the transport of this label into myelin. Frog sciatic nerve as well as mouse nerve was used for these studies, since preliminary in vitro experiments had indicated an incorporation of label into frog nerve phospholipids and the transfer of these into myelin (24).

At the earlier times examined, e.g., 20 min in mouse (Fig. 3 A, B), labeling was heavily concentrated in regions of Schwann cell cytoplasm (arrows) near the level of the Schwann nucleus, but not over the Schwann nuclei (*n*). Heavy labeling was not confined to Schwann cells, but could be seen in other regions such as blood vessels walls

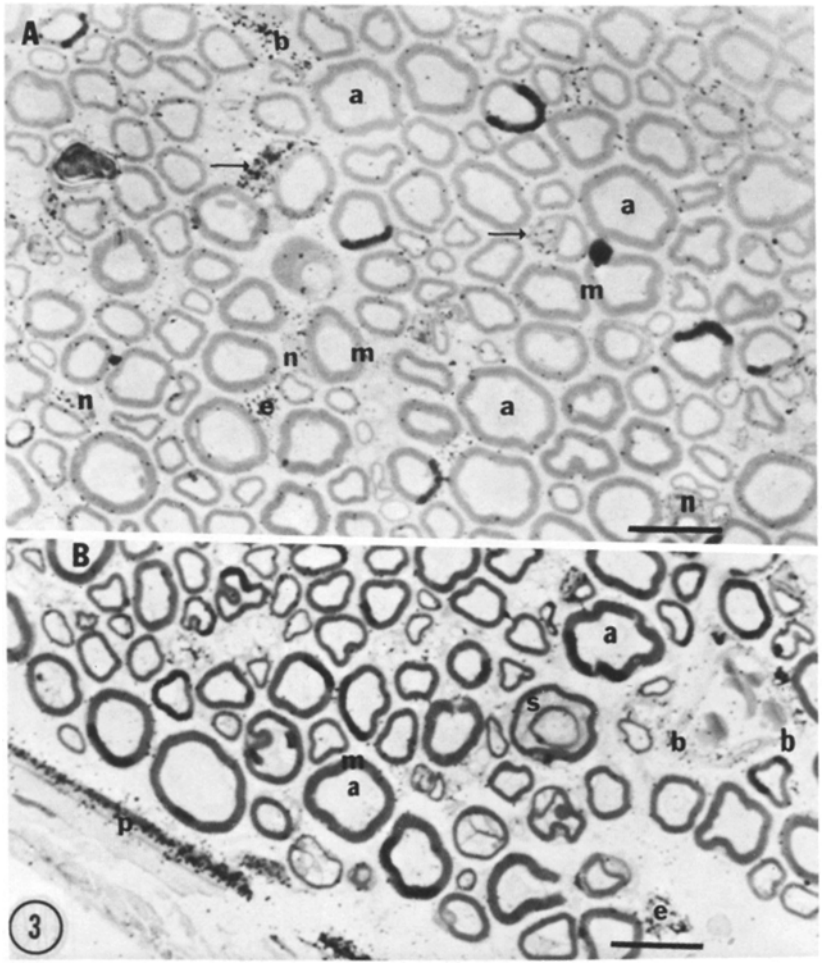

FIGURE 3 Light microscope autoradiographs of cross-section of mouse sciatic nerve fixed at 20 min after labeling with [^{3}H]choline. Exposure, 62 days; × 1,250. Symbols: Axon (*a*), myelin (*m*), Schwann cytoplasm (arrow), Schwann nucleus (*n*), endoneural (*e*), Schmidt-Lantermann cleft (*s*), blood vessel (*b*), perineurial cell layer (*p*). Bar represents 10 μm. Dark bands over some selected areas of myelin are staining artefacts.

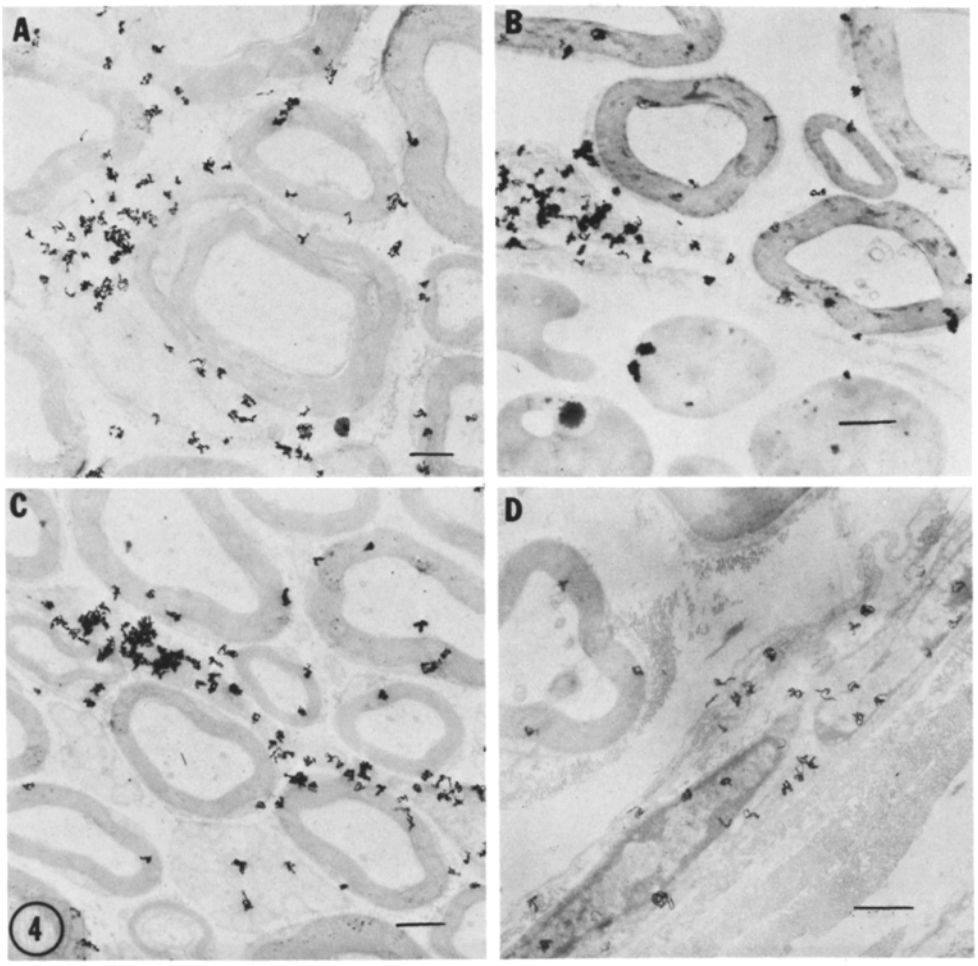

FIGURE 4 Electron microscope autoradiographs of cross-section of mouse sciatic nerve fixed 20 min after labeling with [^{3}H]choline. Exposure 27 days. (A) × 5,300; (B) × 6,600; (C) × 5,300; (D) × 6,600. Bar represents 1 μm.

(Fig. 3 A and B, symbol *b*), perineurium (Fig. 3 B, symbol *p*), and probably endoneural cells (Fig. 3 A, B, symbol *e*). Negligible labeling was seen over axons (*a*), myelin (*m*) or in regions with Schmidt-Lantermann clefts (Fig. 3 B, symbol *s*).

These observations were confirmed at the electron microscope level, where silver grains were localized in Schwann cell cytoplasm excluding nuclear regions (Fig. 4 A), and in regions of blood vessel walls (Fig. 4 B), regions with endoneurium and epithelial cell cytoplasm (Fig. 4 C), and areas surrounging the fibers composed of perineurial cells (Fig. 4 D). At these early times labeling in myelin, axons (Fig. 4 A–D), and regions of Schmidt-Lantermann clefts (Fig. 4 A) was not significant.

At intermediate times, the labeling in Schwann cell cytoplasm was still quite high (Fig. 5 A and C), although much denser labeling appeared over the myelin. In a very few instances, perhaps where nerves were degenerating (Fig. 5 A, symbol *d*), heavy labeling was noticed over the axon. Most axons appeared relatively free of label (Fig. 5 A–C). Some labeling over unmyelinated fibers was observed at intermediate times (Fig. 5 B) and label present in the perineurium at earlier times persisted (Fig. 5 B). Some labeling appeared at the myelin/axon interface (Fig. 5 B–C, arrowheads), which may be related to an adaxonal synthesis (39).

At much later times after injection, as at 35 days in mouse nerve (Fig. 5 D), label was heavily

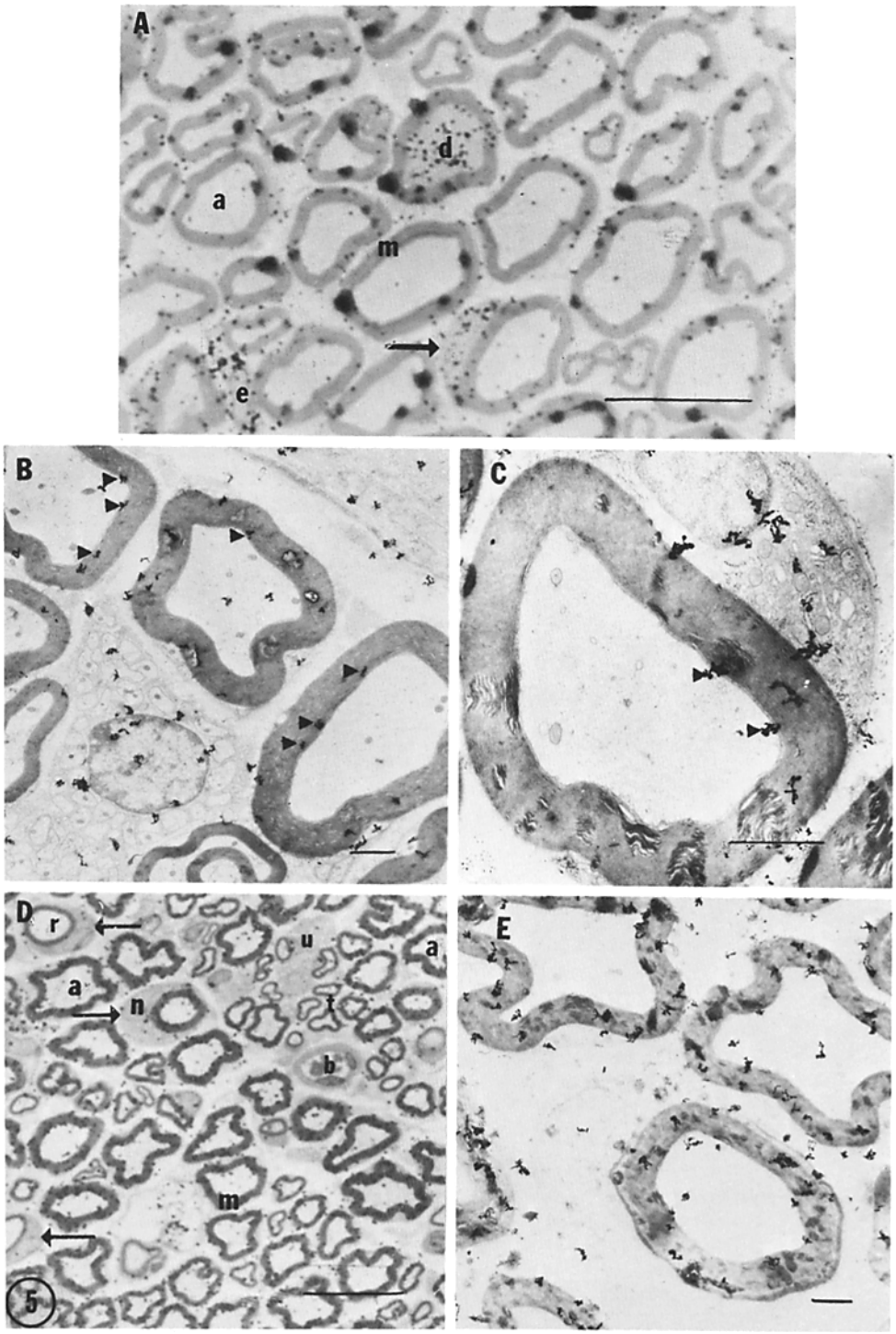

FIGURE 5 Light and electron microscope autoradiographs of transverse sections of nerve fixed at 1 day (A, B, and C) and 35 days (D, E) after injection. (A) Light micrograph exposed for 62 days. × 2,000. (B) EM autoradiograph exposed for 73 days. × 5,300. (C) Same as B. × 12,800. Symbols as in Fig. 3, plus degenerating nerve (*d*), unmyelinated fiber (*u*), thinly myelinated fibers (*t*) and remyelinating fibers (*r*). Arrow heads (B and C) represent grains at or near myelin/axon interface. Bars (A, D) represent 10 μm, and (B, C and E) represent 1 μm.

concentrated over thickly myelinated fibers (*m*) and very little was present anywhere else. Regions of Schwann cell cytoplasm (arrows), blood vessels (*b*), thinly myelinated (*t*), remyelinated fibers (*r*) and unmyelinated fibers (*u*) showed almost no labeling at all. These results were also apparent in electron microscope autoradiographs (Fig. 5 E), where labeling was found largely confined to the myelin of large caliber fibers, and not in cytoplasm.

Quantitation of the Labeling of the EM Autoradiographs

Sample analyses of data taken from mouse nerve fixed at 20 min and 35 days after injection are presented in Table II. The morphological categories chosen for the analyses are listed in the left hand column (Item). Categories 1–7 are discrete areas of the nerve: grains and circles localized to one item were expressed here. Categories 8–14 include grains and circles overlying more than one major category.

A comparison of an early and late sampling time reveal marked changes in grain density over many of the items. In the Schwann cell cytoplasm (item 3), the label starts with high density, 7.12, and falls to 0.61. In the myelin (item 2), label begins low, 0.58, and rises to substantial density, 2.44. The change in label density of the junctional regions fell usually between the densities of the component part, i.e., those items with Schwann cell cytoplasm decreased, and those with myelin increased. No analysis of these junctional elements was made (55, 56) to test if augmented grain densities could be related to specific thin membrane areas as Schwann outer plasma membrane or adaxonal plasma membrane. Grain densities in regions adjacent to highly labeled sources are probably elevated due to scatter from the "hot" sources. For example, junctional regions of Schwann/myelin and Schwann/extracellular space are elevated at early times relative to myelin/extracellular space, due largely to the "hot" Schwann cytoplasm.

A more informative picture of formation and movement of lecithin is obtained by considering labeling intervals between 20 min and 35 days in mouse nerve, or 4 days and 15 days in frog nerve (Tables V and VI). As few grains and little surface area were recorded in categories such as Schwann cell nucleus and other cells, e.g. endoneural cells, changes in these densities were not included in the tables. Junctional items were also eliminated from this table because changes associated with them most probably reflect changes of their component elements. In the mouse, small decreases in cytoplasmic labeling were observed in the first day, with marked decreases occurring at later times. In the frog nerve, at times earlier than 4 days, the labeling was highly localized in Schwann cell cytoplasm. At 4 days, the label in frog Schwann-cell cytoplasm was still considerable, although a marked decrease occurred over the ensuing 4-day period. In both mouse and frog nerve regions of

TABLE V

Grain Density Distributions of a Sequence of E. M. Autoradiographs Demonstrating Movements of Choline-Lipids within Peripheral Nerve

	Mouse						Frog		
Time after injection: 20 min	1 h	4 h	1 day	4 day	35 day	4 day	8 day	15 day
Major items:									
Schwann cytoplasm	7.13	4.95	6.72	4.90	1.35	0.62	9.50	1.86	1.50
Axon	0.18	0.25	0.25	0.36	0.39	0.45	0.19	0.23	0.33
Myelin	0.59	0.72	0.81	1.50	1.51	2.43	1.04	1.41	1.38
Unmyelinated fibers	1.12	1.88	2.83	1.20	0.92	0.24	1.25	0.89	0.92
Extracellular space (E.C.S.)	0.91	0.67	0.71	0.63	0.825	0.25	0.99	0.67	0.57
Significance	0.001	0.001	0.001	0.001	0.001	0.001	0.001	0.001	0.001

Analyses of electron microscope autoradiographs are presented for mouse and frog nerves fixed at indicated times after the injection. Several categories containing less than 5% of the grains and/or random circles as well as all junctional items have been eliminated to simplify this table. The results are expressed as normalized grain densities, and are based on results from grains and circles only associated with the listed categories.

TABLE VI

Grain Density Distributions of a Sequence of E. M. Autoradiographs Demonstrating a Movement of Choline-Lipids into and across Myelin Sheath

	Mouse						Frog		
Time after injection:	20 min	1 h	4 h	1 day	4 day	35 day	4 day	8 day	15 day
Major items:									
Schwann/ECS	3.5	2.5	2.0	1.1	1.4	0.3	2.3	1.1	0.8
Myelin/ECS	1.1	1.2	1.5	0.9	1.1	0.7	1.5	0.9	1.0
Myelin/Schwann	3.7	2.4	2.2	2.3	1.4	1.0	2.2	1.9	1.5
Myelin classes									
1 (outer)	1.5	1.0	1.4	1.4	1.0	1.0	1.6	1.2	1.3
2	0.9	0.6	0.7	1.3	1.0	1.4	1.2	1.3	1.2
3	0.4	0.4	0.2	0.8	1.0	1.4	0.6	1.0	0.9
4	0.1*	0.3*	0.2*	0.9	0.9*	1.5	0.2	0.6	0.9
5 (inner)				0.6		1.4	0.1	0.6	0.8
Myelin/axon	0.4	0.3	0.4	0.4	0.7	0.7	0.4	0.7	0.6

Analyses are presented as in Table V. Normalized grain densities were calculated from only those categories which would reflect a movement of label into and across the myelin lamellae.

* Values recorded in categories 4 and 5 were combined because of limited number of large caliber fibers examined.

high labeling were densely covered with grains at the early sampling times. Overexposure in these regions probably resulted in an underestimation of their grain density.

Significant labeling of myelin is noted even at the shortest labeling times. The grain density over myelin increased to become the highest labeled component at 35 days. In the frog nerve, increases in labeling in myelin are less pronounced. Changes in other major items are less striking compared with Schwann cell cytoplasm and myelin. Labeling over unmyelinated fibers (mouse) peaked at 4 h and decreased markedly thereafter. Slight increases noted in labeling of axon may be real or may be due to scatter from heightened labeling of inner myelin lamellae (see Table VI).

For a more quantitative resolution of the labeling patterns, myelin was considered as being divided into bands of 2,500 Å thickness (Table VI). This value is similar to one chosen by Rawlins of 1,600 Å (38 see 5, 43). The bands extend from the most exterior boundary of the myelinated fiber to the myelin-axon boundary at some cross section distant to a large area of Schwann cell cytoplasm. The grain density decreased with time in the outermost regions of both the mouse (3.5–0.3) and frog (2.3–0.8) fibers and increased in the deeper layers of the thick myelin sheaths. In the mouse, in layer 4 (farther than 7,500 Å from the surface) no grains were seen over the first 4 h, and increased labeling took place from 4 h to the maximum time considered, 35 days. Even at 1 day, labeling in outer layers (1 and 2) was increased compared with inner layers. In the frog, the label in layer 5 was still negligible at 4 days and then increased markedly at 8–15 days. Increases in grain density in the myelin/axon junction and in axon (Table V) may be a result of this inward movement.

DISCUSSION

The concept that the myelin sheath is formed from a proliferation of Schwann (glial) cell plasma membrane originated with the pioneering electron microscope studies of Geren (22) and Robertson (41). More recently, Friede and Samorajski (21) and Webster (54) have done careful morphological investigations which suggest that growth of the myelin sheath occurs at the region of the outer mesaxon. Biochemical studies of lecithin metabolism in brain (28, 31, 50) and tissue culture (27) have indicated that myelin metabolism of this component does not cease in the adult. The studies presented here suggest that, in peripheral nerve, lecithin formed in the Schwann cytoplasm is transferred into myelin through outer layers of the sheath. This result is consistent with the concept that turnover of myelin constituents, such as lecithin, may be mediated through the outer mesaxon or through the surfaces of Schwann cell plasma membrane adjacent to this structure and in contact with both compacted myelin and Schwann cell cytoplasm.

In this discussion, reference will be made to the movement of lecithin rather than, perhaps more correctly, to the movement of ^{3}H-choline-labeled phospholipids. In the shorter term labeling studies, certainly over 90% of the labeling observed is in lecithin. Even at 35 days the activity present in sphingomyelin had not risen greatly (Fig. 2). The slower rate of turnover of sphingomyelin which we observed in PNS myelin parallels the slower turnover of sphingomyelin as compared with lecithin in CNS myelin (29, 50).

It should also be emphasized that the degree of labeling of a component observed in a particular area of an autoradiograph depends both on the rate of turnover and concentration. Thus, the comparative absence of labeling of choline phospholipids in a particular region could be a result of either a much slower turnover of the lipid or a dearth of such lipid in a particular area, so that even rapid turnover would not result in appreciable labeling. Nevertheless, changes in labeling in a region in serial autoradiographs do indicate a net movement or exchange of lipid material to or from the area, although in areas of low phospholipid content labeling would not be observed unless very high levels at radioactivity were produced in these areas.

Lecithin synthesis is likely to occur largely in the endoplasmic reticulum. Transfer to other membranes and organelles is probably mediated through soluble lipoprotein factors present in the cell sap. Studies in brain have demonstrated these factors (35, 37) but the transfer to phospholipids from isolated brain microsomes to myelin particles has not been demonstrated (35). If the transfer process is confined to a limited region of the sheath, as the mesaxon, and subsequent incorporation into the sheath is accomplished largely through lateral diffusion of molecules along the lipid bilayers of the sheath, then this could explain the lack of success of biochemical studies attempting to demonstrate transfer between microsomes and myelin.

Lateral diffusion studies by Kornberg and McConnell (30) provided information on velocities for phospholipids in the plane of a bilayer of greater than 0.05 μm/s. In recent studies (16, 32, 44), lateral diffusion constants for spin-labeled phospholipids have been determined to be 2–20 $\times$ 10^{-8} cm^2/s at 40°C.

For lecithin molecules entering myelin from outer Schwann cell cytoplasm, diffusion through the sheath will depend on the linear distance inward (d) and the time ($t_{1/2}$) in which the labeling in the innermost layers attains one-half the level of the outer layers. According to Dainty and House (14), the diffusion constant, D, can be calculated as, $D = 0.38d^2/t_{1/2}$. For the largest axons having a 6 μm diameter, this distance is 4×10^3 μm (54). Table VI shows half-times for the mouse nerve to be 1 day, and for the frog nerve to be 8 days, corresponding to diffusion constants of 70×10^{-8} cm^2/s and 9×10^{-8} cm^2/s. These values are probably overestimates because the distances for most myelin sheaths would be less than 4×10^3 μm, and the diffusion is dependent on the square of this term. Additional errors may be introduced because the quantitative analyses did not include correction for scatter, and because the values of grain density at the outermost surface (Table VI, category 1) is evaluated from data on sheaths of widely varying sizes. Nevertheless, our diffusion constants for lecithin are compatible with those reported for lecithin in bilayers and sarcoplasmic reticulum (16, 32, 44).

The mechanism of lecithin uptake by peripheral nerve myelin appears to be different from the mechanism of cholesterol uptake (39). Using refined autoradiographic methods, Rawlins (38) found that preformed cholesterol entered the myelin membrane from both the Schwann cell and axolemma regions in 10-day old mice. He concluded furthermore that cholesterol was incorporated into the sheath so rapidly that, within 3 h after injection, it was equilibrated throughout the lamellae of even the largest fibers. One possible explanation for his finding is that in developing animals the amount of Schwann cell cytoplasm inside the myelin is greater than in the adult and label is exchanged through the region of the inner mesaxon as well as the outer mesaxon. The distances the label would have to move would be less than in adult animals. The rapid movement of cholesterol in the myelin membrane itself probably signifies a very rapid diffusion of this molecule into the membrane which is in line with much previous evidence showing rapid exchangeability of this sterol between biological lipoprotein structures (10, 51). In other studies Singer and his co-workers (46–48) have reported rapid movement of proteins and RNA across amphibian myelin.

Rawlins (38) suggested that the transaxonal incorporation of label may be a result of fast axoplasmic flow. Other workers (18, 23) have considered the axonal origin of specific protein components of the myelin membrane, although

Elam (18) restricted his studies to a specific myelin protein of goldfish optic nerve. Autilio-Gambetti et al. (4), have used differential labeling procedures to indicate that the major CNS myelin proteins are synthesized largely by glia elements, and are not of neuronal origin.

Studies by Miani (33), and more recently by Abe et al. (1), have suggested a proximal-distal movement of phospholipids along the nerve. Our studies, aimed at demonstrating axoplasmic movement of lecithin to myelin by measuring the distribution of label along the sciatic nerve after a nonspecific labeling procedure, indicate that this mechanism is at most of minor significance. Supporting this contention are unpublished observations (J. S. Kelly and R. M. Gould) which have demonstrated very low levels of radioactive lipid along peripheral nerve between 4 and 15 days after injection of [^{3}H]choline into a rat cervical dorsal root ganglion.

Singer and co-workers (46–48) have used autoradiography results to argue that glia cells may contribute labeled precursors to the axons. Our experiments have consistently shown only very low labeling of the axonal phospholipids, although it must be admitted that with the low concentration of the lipids in axoplasm (17) the sensitivity of our procedure may not be sufficient to demonstrate such a movement. In addition, labeled lipids entering the axon may be transported rapidly along the axon from the site of entry and not be recorded in autoradiographs prepared near the site of injection. The only times that we have observed high labeling in the axon was in nerves undergoing degeneration (Fig. 5 A). The high labeling during nerve degeneration should come under consideration when measurements of distribution of label distal to a cut nerve are reported (46, 47).

Singer (49) has postulated the possible involvement of the Schmidt-Lantermann cleft in facilitating the movement of constituents through the myelin sheath. At no time after injection do we find prominent labeling of choline phospholipid within these structures. Moreover, if lecithin were transported through the myelin sheath via these clefts, we should expect more rapid rates (49) of appearance of labeled lecithin in inner layers.

Lecithin synthesis from choline precursors occurs in Schwann cell cytoplasm, endoneural cells, blood vessel membranes, and in the cell layers at the innermost part of the peripheral epithelia of the perineurium. This latter structure alone is heavily labeled when label is applied to the surface of the nerve; it may act as a permeability barrier (3) to the uptake of precursors by the nerve.

In summary, the results presented suggest that myelin choline lipids are made, largely if not exclusively, in the glial cell cytoplasm. Transfer from sites of synthesis into myelin may be limited to specific sites on the outer portions of the sheath. This process may be responsible for a fast turnover rate associated with myelin constituents. Once the lipid is associated with the myelin lamellae, the subsequent movement inward is a relatively slow process, most probably mediated by lateral diffusion through the myelin lipid bilayer over very extended surface areas. The vast areas of membrane in myelin surrounding large-caliber fibers suggests that weeks to months may be required to clear molecules completely from the inner surfaces. Additional factors may be responsible for the even lower turnover rates of other myelin constituents, e.g., sphingomyelin.

The authors are indebted to Mr. L. Jarvis for his continued help with light microscope autoradiography and to Dr. Peter Wooding and Mrs. Yvonne Mangnall for their help and advice with electron microscope autoradiography. In addition, improvements in the microinjection techniques were possible through the help and criticism of Doctors Susan H. Standring, Norm Gregson, and John Kelly. The technical assistance of Andrew Letcher and Jane Maddow is here gratefully acknowledged. Valuable discussions with Dr. M. A. Williams, and critical reading of the manuscript by Doctors L. Bachmann and M. Salpeter proved invaluable in organizing and describing quantitative aspects of the electron microscope autoradiography.

A major part of this work was supported by a fellowship to R.M.G. from the Wellcome Trust, and carried out at Cambridge.

Received for publication 3 July 1975, and in revised form 16 October 1975.

REFERENCES

1. ABE, T., T. HAGA, and M. KUROKAWA. 1973. Rapid transport of phosphatidylcholine occurring simultaneously with protein transport in the frog sciatic nerve. *Biochem. J.* **136**:731–740.
2. ADAMS, C. W. M., and O. B. BAYLISS. 1968. Histochemistry of myelin. VI. Solvent action of acetone on brain and other lipid-rich tissues. *J. Histochem. Cytochem.* **16**:115–118.
3. AKER, F. D. 1972. A study of hematic barriers in

peripheral nerves of albino rabbits. *Anat. Rec.* **174**:21–37.

4. AUTILIO-GAMBETTI, L., P. GAMBETTI, and B. SHAFER. 1975. Glial and neuronal contributions to proteins and glycoproteins recovered in myelin fractions. *Brain Res.* **84**:336–340.
5. BACHMANN, L., and M. M. SALPETER. 1965. Autoradiography with the electron microscope: a quantitative evaluation. *Lab. Invest.* **14**:1041–1053.
6. BAILEY, N. T. J. 1959. Statistical Methods in Biology. John Wiley and Sons, Inc., New York. 52–77; appendix 3, p. 194.
7. BARTLETT, G. R. 1959. Phosphorus assay in column chromatography. *J. Biol. Chem.* **234**:466–468.
8. BENES, F., J. A. HIGGINS, and R. J. BARRNETT. 1973. Ultrastructural localization of phospholipid synthesis in the rat trigeminal nerve during myelination. *J. Cell Biol.* **57**:613–629.
9. BENJAMINS, J. A., and G. M. MCKHANN. 1973. Properties and metabolism of soluble lipoproteins containing choline and ethanolamine phospholipids in rat brain. *J. Neurochem.* **20**:1121–1129.
10. BRUCKDORFER, K. R. and C. GREEN. 1967. The exchange of unesterified cholesterol between human low-density lipoproteins and rat erythrocyte "ghosts." *Biochem. J.* **104**:270–277.
11. BUBIS, J. J., and M. WOLMAN. 1962. Arrangement of cholesterol molecules in the myelin sheath. *Nature (Lond.).* **195**:299.
12. COPE, G. H., and M. A. WILLIAMS. 1969. Quantitative study on the preservation of choline and ethanolamine phosphatides during tissue preparation for electron microscopy. *J. Microsc. (Oxf.)* **90**:31–46.
13. DAHLSTROM, A. 1971. Axoplasmic transport (with particular respect to adrenergic neurons). *Philos. Trans. R. Soc. Lond. B. Biol. Sci.* **261**:325–358.
14. DAINTY, J., and C. R. HOUSE. 1966. 'Unstirred layers' in frog skin. *J. Physiol.* **182**:66–78.
15. DAWSON, R. M. C. 1973. The exchange of phospholipids between cell membranes. *Sub-Cell. Biochem.* **2**:69–89.
16. DEVAUX, P., and H. M. MCCONNELL. 1973. Equality of the rates of lateral diffusion of phosphatidylethanolamine and phosphatidylcholine spin labels in rabbit sarcoplasmic reticulum. *Ann. N.Y. Acad. Sci.* **222**:489–498.
17. DEVRIES, G. H., and W. T. NORTON. 1974. The lipid composition of axons from bovine brain. *J. Neurochem.* **22**:259–264.
18. ELAM, J. S. 1974. Association of axonally transported proteins with goldfish brain myelin fractions. *J. Neurochem.* **23**:345–354.
19. FOLCH, J., M. LEES, and G. H. SLOANE STANLEY. 1957. A simple method for the isolation and purification of total lipids from animal tissues. *J. Biol. Chem.* **226**:497–509.
20. FRIEDE, R. L., and T. SAMORAJSKI. 1967. Relation between the number of myelin lamellae and axon circumference in fibers of vagus and sciatic nerves of mice. *J. Comp. Neurol.* **130**:223–232.
21. FRIEDE, R. L., and T. SAMORAJSKI. 1968. Myelin formation in the sciatic nerve of the rat: a quantitative electron microscopic, histochemical, and radioautographic study. *J. Neuropathol. Exp. Neurol.* **27**:546–570.
22. GEREN, B. B. 1954. The formation from the Schwann cell surface of the myelin in the peripheral nerves of chick embryos. *Exp. Cell Res.* **7**:558–562.
23. GIORGI, P. P., J. A. KARLSSON, J. SJOSTRAND and E. J. FIELD. 1973. Axonal flow and myelin protein in the optic pathway. *Nat. New Biol.* **244**:121–124.
24. GOULD, R. M. 1974. Phospholipid metabolism in the peripheral nervous system: radioautography of the incorporation of newly synthesized phosphatidylcholine into myelin. *Biochem. Soc. Trans.* **2**:978–979.
25. HALL, S. M., and N. A. GREGSON. 1971. The *in vivo* and ultrastructural effects of injection of lysophosphatidyl choline into myelinated peripheral nerve fibres of the adult mouse. *J. Cell Sci.* **9**:769–789.
26. HAYAT, M. A. 1972. Basic Electron Microscopy Techniques. Van Nostrand Reinhold Company, New York. 100.
27. HENDELMAN, W. J., and R. P. BUNGE. 1969. Radioautographic studies of choline incorporation into peripheral nerve myelin. *J. Cell Biol.* **40**:190–208.
28. JUNGALWALA, F. B., and R. M. C. DAWSON. 1971. The turnover of myelin phospholipids in the adult and developing rat brain. *Biochem. J.* **123**:683–693.
29. JUNGALWALA, F. B. 1974. The turnover of myelin phosphatidylcholine and sphingomyelin in the adult rat brain. *Brain Res.* **78**:99–108.
30. KORNBERG, R. D., and H. M. MCCONNELL. 1971. Lateral diffusion of phospholipids in a vesicle membrane. *Proc. Natl. Acad. Sci. U.S.A.* **68**:2564–2568.
31. LAPETINA, E. G., G. G. LUNT, and E. DEROBERTIS. 1970. The turnover of phosphatidylcholine in rat cerebral cortex membranes *in vivo*. *J. Neurobiol.* **1**:295–302.
32. MCCONNELL, H. M., P. DEVAUX, and C. SCANDELLA. 1972. Lateral diffusion and phase separations in biological membranes. *In* Membrane Research. C. Fred Fox, editor. Academic Press, Inc. New York. 27–37.
33. MIANI, N. 1964. Proximal-distal movement of phospholipids in the axoplasm of the intact and regenerating neurons. *Prog. Brain Res.* **13**:115–126.
34. MILLER, E. K., and R. M. C. DAWSON. 1972. Can mitochondria and synaptosomes of guinea-pig brain synthesize phospholipids? *Biochem. J.* **126**:805–821.
35. MILLER, E. K., and R. M. C. DAWSON. 1972. Exchange of phospholipids between brain membranes *in vitro*. *Biochem. J.* **126**:823–835.
36. NORTON, W. T., and S. E. PODUSLO. 1973. Myelination in rat brain: methods of myelin isolation. *J. Neurochem.* **21**:749–757.
37. O'BRIEN, J. S., E. L. SAMPSON, and M. B. STERN.

1967. Lipid composition of myelin from the peripheral nervous system. *J. Neurochem.* **14**:357–365.

38. RAWLINS, F. A. 1973. A time-sequence autoradiographic study of the *in vivo* incorporation of (1,2-^{3}H) cholesterol into peripheral nerve myelin. *J. Cell Biol.* **58**:42–53.
39. RAWLINS, F. A. 1974. Localization of ^{3}H-choline incorporated *in vivo* into myelin. Eighth International Congress on Electron Microscopy, Canberra, vol. 2. 288–289.
40. REYNOLDS, E. S. 1963. The use of lead citrate at high pH as an electron opaque stain in electron microscopy. *J. Cell Biol.* **17**:208–213.
41. ROBERTSON, J. D. 1955. The ultrastructure of adult vertebrate peripheral myelinated nerve fibers in relation to myelinogenesis. *J. Biophys. Biochem. Cytol.* **1**:271–278.
42. ROOZEMOND, R. C. 1969. The effect of fixation with formaldehyde and glutaraldehyde on the composition of phospholipids extractable from rat hypothalamus. *J. Histochem. Cytochem.* **17**:482–486.
43. SALPETER, M. M., L. BACHMANN, and E. E. SALPETER. 1969. Resolution in electron microscopic autoradiography. *J. Cell Biol.* **41**:1–20.
44. SCANDELLA, C. J., P. DEVAUX, and H. M. MCCONNELL. 1972. Rapid lateral diffusion of phospholipids in rabbit sarcoplasmic reticulum. *Proc. Natl. Acad. Sci. U.S.A.* **69**:2056–2060.
45. SHELTAWY, A., and R. M. C. DAWSON. 1966. The polyphosphoinositides and other lipids of peripheral nerves. *Biochem. J.* **100**:12–18.
46. SINGER, M., and M. M. SALPETER. 1966. The transport of ^{3}H-l-histidine through the Schwann and myelin sheath into the axon, including a reevaluation of myelin function. *J. Morphol.* **120**:281–315.
47. SINGER, M., and M. R. GREEN. 1968. Autoradiographic studies of uridine incorporation in peripheral nerve of the newt, Triturus. *J. Morphol.* **124**:321–344.
48. SINGER, M. 1968. Penetration of labelled amino acids into the peripheral nerve from surrounding body fluids. *In* Growth of the Nervous System. G. E. W. Wolstenholme and M. O'Connor, editors. Little Brown & Company, Boston. 200–219.
49. SINGER, M. and S. V. BRYANT. 1969. Movements in the myelin Schwann sheath of the vertebrate axon. *Nature (Lond.).* **221**:1148–1150.
50. SMITH, M. 1968. The turnover of myelin in the adult rat. *Biochim. Biophys. Acta.* **164**:285–293.
51. SMITH, R. J. M., and C. GREEN. 1974. The rate of cholesterol 'flip-flop' in lipid bylayers and its relation to membrane sterol pools. *FEBS (Fed. Eur. Biochem. Soc.) Lett.* **42**: 108–111.
52. STEIN, O., and Y. STEIN. 1969. Lecithin synthesis, intracellular transport and secretion in rat liver. IV. A radioautographic and biochemical study of choline-deficient rats injected with choline-^{3}H. *J. Cell Biol.* **40**: 461–483.
53. STEIN, O., and Y. STEIN. 1971. Light and electron microscopic radioautography of lipid techniques and biological application. *In* Advances in Lipid Research, Vol. 9. R. Paoletti and D. Kritchevsky, editors. Academic Press, Inc., New York. 1–72.
54. WEBSTER, H. DEF. 1971. The geometry of peripheral myelin sheaths during their formation and growth in rat sciatic nerves. *J. Cell Biol.* **48**:348–367.
55. WILLIAMS, M. A. 1969. The assessment of electron microscopic autoradiographs. *In* Advances in Optical and Electron Microscopy, Vol. 3, R. Barer and V. E. Cosslett, editors. Academic Press, Inc. New York. 219–272.
56. WILLIAMS, M. A. 1973. Electron microscopic autoradiography: Its application to protein biosynthesis. *In* Techniques in Protein Biosynthesis, Vol. 3. P. N. Campbell and J. R. Sargent, editors. Academic Press, Inc., New York. 126–190.
57. WIRTZ, K. W. A. 1974. Transfer of phospholipids between membranes. *Biochim. Biophys. Acta.* **344**:95–117.